HGT

Inflammation-Inducible Expression of Human Indoleamine 2,3-Dioxygenase Driven by the E-Selectin Promoter Ameliorates Collagen-Induced Arthritis

Mehmet Karaçay,[1,2] İzel Yılmaz,[1] Ayşe Özden Barazi Soydaş,[3] Gökçen Güvenç-Bayram,[4] Figen Ersoy,[5] Cansel Güzin Özgüden Akkoç,[6] Arzu Yılmaztepe Oral,[7] Ahmet Akkoç,[8] Murat Yalçın,[9] and Haluk Barbaros Oral[10,*]

[1]Department of Medicine-Immunology, Institute of Health Sciences, Bursa Uludag University, Bursa, Türkiye; [2]Division of Medical Genetics, Department of Internal Medicine, Faculty of Medicine, Van Yuzuncu Yil University, Van, Türkiye; [3]Department of Immunology, Graduate School of Health Sciences, Gazi University, Ankara, Türkiye; [4]Department of Physiology, Faculty of Veterinary Medicine, Dokuz Eylul University, Izmir, Türkiye; [5]Department of Molecular Biology and Genetics, Bursa Uludag University, Bursa, Türkiye; [6]Department of Histology and Embryology, Faculty of Veterinary Medicine, Bursa Uludag University, Bursa, Türkiye; [7]Department of Medical Biochemistry, Faculty of Medicine, Bursa Uludag University, Bursa, Türkiye; [8]Department of Pathology, Faculty of Veterinary Medicine, Bursa Uludag University, Bursa, Türkiye; [9]Department of Physiology, Faculty of Veterinary Medicine, Bursa Uludag University, Bursa, Türkiye; and [10]Department of Immunology, Faculty of Medicine, Bursa Uludag University, Bursa, Türkiye.

Rheumatoid arthritis is a chronic autoimmune disease characterized by persistent synovial inflammation and progressive joint destruction. Although biological disease-modifying anti-rheumatic drugs (DMARDs) have transformed treatment, their systemic immunosuppression, high cost, and incomplete efficacy in certain joints remain significant challenges. To address these limitations, we developed a localized gene therapy using the human indoleamine 2,3-dioxygenase (*hIDO*) gene driven by the E-selectin (ELAM-1) promoter, which is responsive to inflammatory cytokines. We assessed ELAM-1 promoter responsiveness to interleukin-1β (IL-1β) stimulation *in vitro* mainly using the HeLa cell line, measuring *hIDO* expression and enzymatic activity by enzyme-linked immunosorbent assay, quantitative reverse transcription-polymerase chain reaction (qRT-PCR), Western blotting and kynurenine assays. *In vivo*, we established a robust collagen-induced arthritis (CIA) model in BALB/c mice, which are normally resistant to CIA, and delivered pELAM-1pro/hIDO plasmids intra-articularly via liposomes. Therapeutic efficacy was evaluated by clinical scoring, ankle circumference, histopathology, immunohistochemical quantification of synovial $CD4^+$ T cells and $CD68^+$ macrophages, and endpoint immunohistochemical assessment of IDO expression. *In vitro*, the ELAM-1 promoter allowed rapid, high-level expression of hIDO within 2 h of IL-1β stimulation, without IDO-induced suppression of the promoter. *In vivo*, pELAM-1pro/hIDO treatment significantly reduced ankle swelling and clinical arthritis scores more rapidly than constitutive CMV-driven hIDO, achieving marked histological improvement on day 7. The treated joints exhibited substantial reductions in pathogenic $CD4^+$ T cells and $CD68^+$ macrophages, consistent with the IDO immunoregulatory mechanism. This study supports the feasibility of a localized gene therapy approach using an inflammation-responsive promoter and suggests localized immunomodulation at disease sites in a manner consistent with inflammation-associated promoter activity.

Keywords: rheumatoid arthritis, E-selectin promoter, indoleamine 2,3-dioxygenase, gene therapy

INTRODUCTION

Rheumatoid arthritis (RA) is an autoimmune disease with persistent inflammation of the synovial joints, which ultimately leads to the invasion and destruction of articular cartilage and bone. The immunopathology of RA is initiated by the presentation of citrullinated self-antigens or cross-reactive foreign peptide antigens by antigen-presenting cells (APCs) to naive T cells in lymph nodes.[1,2] After recognition of self-antigens in the presence of co-stimulatory molecules, such as CD80 and CD86, T cells become activated and differentiated into self-antigen-specific effector helper T (Th) cells, including Th1, Th17, Th22, or T follicular helper (Tfh) cells.[2] Th1 and Th17 cells migrate to the synovial membrane and produce pro-inflammatory cytokines (IFN-γ and IL-17), which result in the production of several chemokines (CXCL1, CXCL2, CXCL8, CCL2, CCL7, and CCL20) and pro-inflammatory cytokines (TNF-α, IL-1β, and IL-6) from cartilage,

*Correspondence: Prof. Haluk Barbaros Oral, Department of Immunology, Faculty of Medicine, Bursa Uludag University, Nilüfer, Bursa 16059, Türkiye. E-mail: oralb@uludag.edu.tr

© The Author(s)
DOI: 10.1177/10430342261452520

synovial cells, bone cells, and macrophages.[3,4] Additionally, autoreactive Tfh cells initiate the differentiation of B cells into plasma cells, which leads to the production of specific antibodies against self-antigens. Subsequently, these autoantibodies accumulate in the synovium and form immunocomplexes that also cause bone and cartilage degradation by activating the complement system and macrophages.[5]

Currently, several synthetic and biological disease-modifying anti-rheumatic drugs (DMARDs) have been developed and approved for the treatment of RA. Systemic administration of these drugs has been beneficial in a dose-dependent manner, particularly in early-onset RA.[6,7] However, these drugs have relatively short half-lives, requiring frequent administration, increasing treatment costs, and systemic side effects.[3,4,8] Moreover, certain joints may remain refractory to therapy despite control of systemic disease. For instance, despite overall systemic disease control achieved with biological DMARDs such as TNF-α inhibitors (*e.g.,* infliximab or adalimumab) and IL-6 receptor antagonists (*e.g.,* tocilizumab), certain joints may remain partially refractory to treatment,[6,7] highlighting the need for localized precision immunomodulation.[9]

Indoleamine 2,3-dioxygenase (IDO) is an enzyme that catalyzes the degradation of tryptophan to kynurenine and its derivatives. IDO was first defined by its contribution to maternal-fetal immune tolerance.[10] Therefore, it has been demonstrated that the IDO-dependent metabolic pathway is part of a very simple and evolutionarily conserved immune tolerance mechanism. Some *in vivo* studies in homozygous mice (*IDO-/-*KO) lacking the IDO gene have shown that the IDO enzyme does not play a role in central tolerance.[11] However, several *in vivo* studies have shown that IDO significantly contributes to acquired peripheral tolerance.[12–15] IDO-dependent tryptophan degradation has been demonstrated to cause inhibition and apoptosis of effector T cells, as well as suppression of the cellular immune response by de novo induction of regulatory T cells.[16–21] Therefore, IDO, a key regulator in both innate and adaptive immunity, can be considered a therapeutic approach for the treatment of inflammatory and autoimmune diseases, as well as organ transplantation.

Local gene therapy for arthritis, using therapeutic genes under the control of inflammation-regulated promoters, represents a promising alternative to reducing the side effects of conventional treatments. These promoters initiate therapeutic gene expression in response to inflammatory signals, which could enhance local regulation of inflammatory activity. Endothelial Leukocyte Adhesion Molecule-1 (ELAM-1), also known as E-selectin, is an adhesion molecule that is expressed within 4–6 h in response to proinflammatory cytokines such as TNF-α and IL-1.[22–25] The ELAM-1 promoter has been used for gene delivery in viral and non-viral vectors. The expression of a gene encoding an anti-inflammatory therapeutic protein under the control of the E-selectin (ELAM-1) promoter has been shown to occur after cytokine stimulation. Unlike constitutive promoters such as CMV or broadly responsive inflammatory promoters, the ELAM-1 promoter has been reported to support localized transgene activity at inflamed endothelial sites, potently reducing systemic exposure compared with constitutive expression systems.[26–29]

In this study, we investigated the therapeutic effect of expressing IDO under the control of the ELAM-1 promoter, which is known to respond to inflammatory cytokine signaling, in our local CIA model.

Here, we report the development of an inflammation-responsive IDO gene therapy under the control of the ELAM-1 promoter, delivered intra-articularly via a non-viral liposomal vector in a collagen-induced arthritis (CIA) model. This design integrates two features: (1) exploitation of IDO's tolerogenic pathway in an inflammation-associated manner, avoiding constitutive overexpression,[30–32] and (2) a delivery system that could be adapted for localized treatment of refractory joints in RA patients,[33–36] potentially reducing systemic exposure and adverse effects. By achieving significant disease modulation in this model, our objective was to evaluate the therapeutic potential of this strategy as a proof-of-concept for locally targeted immunomodulatory approaches in RA.

MATERIALS AND METHODS

Animals

Male BALB/c mice (H-2d), 6–8 weeks of age, were purchased from the Experimental Animal Breeding and Research Centre, Bursa Uludag University, Bursa, Türkiye. Before experiments, mice were housed five per cage under specific pathogen-free conditions at 20°C–22°C and 60%–70% humidity, with a 12 h light/12 h dark cycle, and had *ad libitum* access to standard mouse chow and water. All experimental procedures were conducted in accordance with the National Institutes of Health Guide for the Care and Use of Laboratory Animals and were approved by the Animal Care and Use Committee of Uludağ University (approval no: 2013-06/02).

Experimental design and group allocation

The animals were randomly assigned to the experimental groups. Each group initially consisted of 8 male BALB/c mice (n = 8 per group). For histopathological evaluation (hematoxylin-eosin [H&E]) and semi-quantitative immunohistochemical analyses of CD68 and CD4, the same animals were used at each time point. Consequently, 2 mice per group were sacrificed on day 7, 2 mice per group on day 21, and the remaining 4 mice per

group were sacrificed at the final experimental endpoint (day 28 after treatment; CIA day 49). In contrast, immunohistochemical detection of IDO expression was performed only at the final experimental end point, and representative images are presented. Due to these scheduled sacrifices, longitudinal measurements of ankle circumference were performed after day 21 in the remaining animals ($n = 4$ per group) until the final end point. Clinical and histological evaluations were performed under blinded conditions by two independent observers. No animals were excluded from the study.

Construction of pELAM-1pro/human IDO (*hIDO*) expression vector

The pCMV/hIDO hygro-plasmid was commercially provided by Sino Biological, China.

The ELAM-1 promoter was amplified from human genomic DNA and cloned upstream of the *hIDO* coding sequence to replace the CMV promoter in the parental pCMV/hIDO plasmid. All constructs were sequence-verified. A schematic representation of the cloning strategy and detailed construct information are presented in Supplementary Figure S1A–E).

Plasmid transfection and IL-1β stimulation in HeLa cells and additional cell lines

HeLa cells (2.5×10^5 cells per well) were seeded in 6-well plates and transfected using Lipofectamine 2000 (Invitrogen, USA) according to the manufacturer's instructions. For each well, 4 μg plasmid DNA was complexed with 7.5 μL Lipofectamine 2000 in the ratios recommended by the manufacturer.

Cells were transfected with the pELAM-1pro/hIDO plasmid and subsequently stimulated with IL-1β (2 ng/mL or 5 ng/mL) for 4 or 24 h. During transfection experiments, the pCMV/βgal plasmid was used as a negative control, and pCMV/hIDO was used as a positive control plasmid.

Following the indicated incubation periods, cell lysates were collected in the presence of a protease inhibitor cocktail (Sigma, USA) for downstream analyses (Supplementary Fig. S2A).

IL-1β concentrations (2 and 5 ng/mL) were selected based on preliminary dose–response experiments demonstrating consistent activation of the ELAM-1 promoter within the 2–10 ng/mL range (Supplementary Fig. S3A).

The 5 ng/mL concentration was chosen as a reproducible intermediate dose that reliably induced promoter activation without requiring higher cytokine exposure.

Comparable IL-1β-dependent increases in IDO production were also observed in HEK293 and RAW 264.7 cells after transfection with pELAM-1pro/hIDO, although the transfection efficiency was lower in RAW 264.7 macrophages (Supplementary Fig. S2B and C).

Quantification of IL-1β-induced IDO mRNA expression by RT-qPCR

The expression of IDO mRNA in transfected HeLa cells with different levels of IL-1β (2 ng/mL, 5 ng/mL) and incubation hours (0, 0.5, 1, 2, and 4 h) was detected by qRT-PCR. Total RNA was isolated using the Ez-10 Spin Column Total RNA Minipreps Super Kit (Bio Basic Inc., USA). First-strand cDNA synthesis was performed with the RevertAid First Strand cDNA Synthesis Kit (Fermentas Life Science, USA). F-(5′CAAAGGTCATGGAGATGCC-3′) and R-(5′CCACCAATAGAGAGACCAGG-3′) were the primers for *hIDO*. The glyceraldehyde-3-phosphate dehydrogenase (*GAPDH*) gene primers F-(5′-AGGGCTGCTTTTAACTCTGGT-3′) R-(5′-CCCCACTTGATTTTGGAGGGA-3′) were used as an endogenous control to normalize the differences in cDNA expression levels. The PCR reaction conditions were adjusted to an initial hold at 50°C for 2 min, then 95°C for 10 min, followed by 40 cycles of 15 s at 95°C, 15 s at 55°C, and 15 s at 72°C. The melting curve was checked every 0.3°C for 1 s from 40°C to 94°C to determine whether the primers form dimers. Real-time PCR was performed using SYBR green (SybrGreen JumpStart™ Taq Ready mix; Sigma-Aldrich, St. Louis, MO, USA). PCR mix was conducted with Exicycler96 (Bioneer, Dae-Jeon, Republic of Korea). The fold change of all values was normalized with the *GAPDH* control. The relative expression of the h*IDO* gene was calculated as $2^{-\Delta\Delta CT}$.

Measurement of IDO production by enzyme-linked immunosorbent assay (ELISA)

Sandwich ELISA was used to provide quantitative measurement of hIDO protein levels, using a commercial hIDO protein kit (Cloud Clone Corp., USA) according to the manufacturer's instructions. After the cell transfection process, HeLa cells, as mentioned previously, were stimulated with 2 ng/mL and 5 ng/mL at final IL-1β concentrations and incubated for 24 h. Cell lysates were collected with sterile phosphate-buffered saline (PBS). The freeze–thaw method was used three times at −20°C, and therefore the cell membrane was damaged, and its contents were released into PBS. Cell debris was removed with the help of centrifugation. The supernatant phase was used for the assay. The tests were performed in technical triplicate for each sample and repeated in at least three independent biological experiments, and the concentrations were calculated using standard curves.

Quantification of IDO activity by L-kynurenine production

The enzyme activity of IDO (EC 1.13.11.52) was determined by colorimetric measurement of the concentration of the tryptophan metabolite L-kynurenine.[37] After preparing a Premix (2×) concentration IDO buffer solution

(100 mM PBS, 40 mM Ascorbic acid, 20 μM Methylene blue, 200 μg catalase, and 800 mM tryptophan, pH 6.5), all standards were performed, and the supernatants were diluted with an equal volume of the premix (2×) IDO buffer. They were incubated at 37°C for 30 min. The reaction was stopped at the end of the incubation period by adding 30% TCA (Trichloroacetic acid) solution. Subsequently, a 96-well flat-bottom plate was incubated again at 52°C for 30 min. After incubation, the plate was quickly centrifuged for 30 s, and an equal volume of Erlich solution was added to each well before being incubated at room temperature. About 10 min later, the color change took place, and the plate was evaluated by spectrophotometry at 492 nm. Tests were performed in duplicate for each sample.

Quantification of IDO protein expression by Western blot

HeLa cell lysates were collected and resuspended in lysis buffer radioimmunoprecipitation assay (1×) (Santa Cruz, CA, USA), 200 mM phenylmethylsulfonyl fluoride (Santa Cruz, CA, USA), 100 mM sodium orthovanadate (Santa Cruz, CA, USA), and 45 μL proteinase inhibitor cocktail (Santa Cruz, CA, USA). An equal amount of total protein (35 μg) and the pre-stained protein marker (Cell Signaling, MA, USA) were loaded onto 4%–12% NuPAGE Bis-Tris Mini Gel. Separated proteins were transferred to the Nitrocellulose membrane. The I-Blot gel transfer device (Invitrogen, CA, USA) was used in the transfer process. The transfer process was carried out for 7 min as recommended by the manufacturer. To prevent non-specific bindings, the membrane was blocked for 1 h at room temperature with 5% non-fat dry milk (Cell Signaling, MA, USA). anti-human IDO (D5J4E-Rabbit) mAb (Cell Signaling, MA, USA) was diluted 1:1000 with 5% bovine serum albumin (BSA) and incubated at 4°C for 18 h. Following that, the secondary antibody, anti-Rabbit IgG-horseradish peroxidase (HRP) (7074S-Cell Signaling, MA, USA), was used in 1:2000 dilution 5% BSA and incubated for 1 h. The membrane was kept in a solution containing HRP substrate for 30 s, and then immunoreactivity was detected by Fusion FX-7 (Vilber Lourmat, Torcy, FR). Band intensities were quantified by densitometric analysis using ImageJ (NIH, USA) and normalized to GAPDH. Representative relative IDO/GAPDH intensity values are presented in (Supplementary Fig. S3B).

Induction and therapeutic evaluation in the mouse model of CIA

Type II bovine nasal septum collagen (Sigma-Aldrich, USA No: C7806-10MG) and Freund's adjuvant complete (CFA, *Mycobacterium tuberculosis* heat and killed lyophilized cell powder) (Sigma-Aldrich, USA No: F5881-6X10 mL) were used to create the CIA arthritis model in BALB/c mice.[38] The nasal collagen from the bovine septum was dissolved in 0.1 M acetic acid (Sigma-Aldrich, USA No: 38051-1EA), freshly prepared for injection at a final concentration of 2 mg/mL. The mice were anesthetized with (2%–4%) sevoflurane and 100% O_2. The mice's posterior right paw knee area and back, where the injections were performed, were cleaned with 70% ethanol-soaked cotton. In order to establish a successful and optimal CIA model in BALB/c mice, 0.01 mL (2 mg/mL) of type II collagen emulsion was intra-articularly injected with a 30 G insulin needle syringe into the right paw knee joint of the mouse; following that, 0.1 mL CFA was subcutaneously injected; the left paw of the mice was used as a control. The collagen emulsion and CFA injections were repeated 14 days after the initial induction to boost CIA formation. After the initial injection, arthritis formation was monitored for 21 days, and clinical evaluations were conducted.

The local CIA was evaluated as stated in our previous studies.[39] For this evaluation, clinical arthritis scoring depends on arthritis-induced joint thickness, erythema, and swelling. These evaluations were conducted on days 0, 14, and 21 after the initial dose of collagen emulsion and CFA. An arthritis score between 0 and 4 was given according to the severity of the evaluation criteria.

Intra-articular plasmid delivery and therapeutic evaluation in CIA mice

Conditions that provided the highest gene transfer efficiency were determined as Plasmid DNA (0.5 mg/5 mL) and Lipofectamine 2000 (1.5 mL/5 mL). The green fluorescent protein (GFP) reporter plasmid (pcDNA/GFP; Addgene plasmid #160697) was complexed with Lipofectamine 2000 and injected into the joint cavity of BALB/c mice using an insulin syringe. Joints were harvested 24 h after injection, and tissue sections were subjected to immunohistochemical analysis using an anti-GFP antibody to evaluate the *in vivo* delivery of the plasmid (Fig. 3).

Joint tissues harvested 24 h after intra-articular injection of pcDNA/GFP were processed for immunohistochemical detection of GFP expression. Paraffin-embedded sections were subjected to heat-mediated antigen retrieval and incubated overnight at 4°C with a rabbit anti-GFP primary antibody (Abcam, ab290) diluted 1:500. Detection was performed using a biotin–streptavidin detection system with DAB as chromogen. Hematoxylin was used for counterstaining.

Immunohistochemical detection of IDO

Immunohistochemical staining for IDO was performed on paraffin-embedded joint sections. A rabbit polyclonal anti-IDO antibody (IDO H-110, sc-25808; Santa Cruz

Biotechnology), raised against amino acids 271–380 of human IDO, was used as the primary antibody.

Sections mounted on poly-L-lysine-coated slides were incubated overnight at 37°C prior to staining. After deparaffinization and rehydration, heat-mediated antigen retrieval was performed using citrate buffer (pH 6.0; ab64236, Abcam). The slides were heated in a microwave oven at 600 W for 2×5 min and allowed to cool to room temperature. The sections were washed in PBS.

Endogenous peroxidase activity was blocked using hydrogen peroxide for 15 min, followed by PBS washes. To reduce non-specific binding, sections were incubated with a protein blocking solution according to the manufacturer's instructions.

The primary antibody was diluted 1:100 in antibody diluent (Epredia™ Lab Vision™ Antibody Diluent OP Quanto, Fisher Scientific) and applied overnight at 4°C in a humidified chamber. After incubation, sections were washed with PBS and incubated with a ready-to-use HRP-conjugated secondary antibody (UltraVision Detection System Anti-Polyvalent HRP/DAB, TP-015-HD, Thermo Fisher Scientific) for 30 min at room temperature.

Immunoreactivity was visualized using DAB chromogen, and slides were counterstained with Harris hematoxylin (HHS16, Sigma-Aldrich). Subsequently, the sections were dehydrated, cleared in xylene, and mounted with a permanent mounting medium.

Human pancreatic adenocarcinoma and rat spleen tissues were used as positive controls.

The therapeutic plasmid pELAM-1pro/hIDO and the control plasmids pCMV/hIDO, pCMV/βgal were complexed with Lipofectamine 2000, and the injection of saline was carried out independently as an additional control.

Primary collagen immunization was performed on day 0 with a booster on day 14. Based on the established kinetics of our local BALB/c CIA model, clinical scores and joint swelling peak around day 21 (Guvenc et al., 2018).[39] Therefore, intra-articular plasmid administration was performed on day 21 to evaluate therapeutic rather than preventive efficacy. The animals were then monitored until day 49 to assess sustained effects during the chronic phase of the disease.

The saline and mock plasmid (pCMV/βgal) groups were included to control for injection-related and vector-related effects, respectively, and served as procedural controls for baseline comparison.

BALB/c mice were intentionally selected because their moderate susceptibility to CIA enables reproducible induction of localized chronic inflammation without excessive joint destruction, thus providing an appropriate therapeutic window to evaluate the efficacy of treatment.

Although a separate group injected with sham was not included, saline-only and mock plasmid-treated groups (pCMV/βgal) were used to control for injection and vector-related effects, respectively, and thus served as functional sham controls.

The therapeutic effect was assessed taking into account the change in ankle circumference, clinical and histopathological scoring, and the number of $CD4^+$ T cells infiltrated and $CD68^+$ macrophages.

Clinical arthritis scoring and paw swelling measurements

Treatment was inspected using a clinical arthritis scoring system, and paw swelling was measured with the help of a caliper. Up to day 49, measurements were taken every week (Supplementary Fig. S4A).

Histopathological and immunohistochemical analyses of joint tissues

At each scheduled time point (day 7, day 21, and day 28 after treatment), mice were anesthetized with sevoflurane (2%–4% in 100% O_2) and sacrificed by cervical dislocation under anesthesia. For histological investigation, the hind paw was removed while leaving the knee joint intact. The tissue samples were fixed in a 10% formalin solution for 48 h at 37°C in an incubator. After that, the samples were put in a decalcifying solution (10% ethylenediamine tetra acetic acid) for 14 days. Every other day, the decalcifying solution was replaced. Decalcifying tissues were embedded in liquid paraffin, and a 5-µm tissue section was cut and mounted on 30% lysine glass slides for H&E staining. Histological scoring was performed using a standardized semi-quantitative 0–4 scale based on the severity of synovial inflammation, pannus formation, cartilage damage, and bone involvement. All sections were evaluated independently by two blinded investigators to ensure consistency and minimize observer bias.

IDO immunoreactivity in joint sections was evaluated as described above. Pancreatic adenocarcinoma tissue, previously reported to exhibit strong expression of IDO,[40] was used as a positive control. Mouse spleen tissue was included as a lymphoid reference tissue for validation of IDO immunoreactivity.[41] Negative control sections were processed in parallel by omitting the primary antibody.

The presence of synovial infiltrating $CD4^+$, T lymphocytes, and $CD68^+$ macrophages in tissue sections was demonstrated using the indirect streptavidin-biotin complex method. The decalcified tissue sections were deparaffinized in xylol. The preparations were post-fixed with an alcohol series and washed with PBS. They were boiled in citrate solution (pH 6) for 5 min to extract antigens. To eliminate endogenous peroxidase, they were incubated in 3% H_2O_2 for 10 min. After being washed with PBS, they were incubated with blocking solution for 10 min at room temperature. For 1 h, the tissues were incubated with

1:200 CD4 mAb (clone: EPR19514, Abcam Limited, Cambridge, UK). A mouse spleen tissue section was used as a positive control for CD4 staining. CD68 Ab (ab125212, Abcam Limited, Cambridge, UK) was diluted 1:2000 and incubated for 1 h, bone marrow tissue was used as a positive control for CD68 staining. Negative control sections were processed in parallel by omitting the primary antibody.

The samples were incubated with the secondary antibody at room temperature for 10 min, washed with PBS, and then incubated with DAB chromogen for 3 min. The sections were counterstained with Harris hematoxylin, washed with distilled water, dehydrated using graded alcohols, cleared in xylene, and mounted with coverslips. An immunohistochemical evaluation was performed by two independent observers considering the intensity of stained target cells: non-staining (-), weak staining (+), moderate staining (++), and severe staining (+++), so scoring values were given from 0 to 3.

Light microphotographs were analyzed using a Nikon Eclipse Ni microscope (Tokyo, Japan) equipped with a DS-Fi2 camera and supported by the NIS Elements F 4.00.00 imaging software (Nikon Soft Imaging Solution). Observations were conducted at a magnification of 200×.

Statistical analysis

Statistical analyses were performed with GraphPad Prism 8 (GraphPad Software, CA, USA). Continuous variables, including ELISA measurements, kynurenine production, q-RT PCR fold changes, Western blot densitometry, and ankle circumference values, were analyzed using one-way analysis of variance (ANOVA) followed by Tukey's *post hoc* test. Ordinal data, including clinical arthritis scores, histopathological scores, and immunohistochemical grading, were analyzed using the Kruskal–Wallis test followed by Dunn's multiple comparison test. Data are presented as mean ± standard deviation (SD). A p value < 0.05 was considered statistically significant. Statistical analyses were performed using biological replicates, with sample sizes varying according to time point and analysis, as described in the Experimental design section.

RESULTS

Inducibility of the ELAM-1 promoter by IL-1β stimulation in HeLa cells

The most important approach that adds originality to our study is that the therapeutic gene that may be effective for the treatment of arthritis can only be induced during inflammation. However, the critical potential problem with IDO, which we aim to use as a potential therapeutic gene, is the possibility that IDO may suppress the excitability of the ELAM-1 promoter. There are no published data that clearly and definitively show that IDO suppresses the ELAM-1 promoter. It is also possible that IDO may be an effective immune regulator, although temporarily, until it suppresses the ELAM-1 promoter. Therefore, we investigated whether reporter CAT expression would be affected in HeLa cells co-transfected with pELAM-1pro/CAT plasmid and a CMV promoter-controlled plasmid that constitutively drives IDO expression. In these experiments, pCMV/βgal (instead of pCMV/IDO) was used as a control. The pELAM-1pro/CAT plasmid carries out CAT gene expression during activation of the ELAM-1 promoter (Supplementary Fig. S3A). In this experiment, IDO overexpression did not show a repressive effect on the promoter of ELAM-1, but increased it. Co-transfection research suggested that the use of a plasmid concentration of pELAM-1/CAT that was three times lower than ideal was responsible for lower CAT levels than expected (Supplementary Fig. S3C).

According to an ELISA and IDO activity assay of transfected HeLa cells, *hIDO* expression was significantly upregulated once these cells were transfected with pELAM-1pro/hIDO and stimulated with 5 ng/mL IL-1β for 24 h compared with the negative and unstimulated groups. (Fig. 1A and B). The ELAM-1 promoter activation effect on *IDO* gene expression was also detected with Western blotting analysis. In unstimulated cells, the IDO protein was not detected, while pronounced expression was observed at a dose of 5 ng/mL and in cells transfected with pCMV/hIDO (positive control), due to the CMV (constitutive) promoter region (Fig. 1C).

Because translation and protein accumulation require additional time beyond early transcriptional activation, protein-level validation was performed at 24 h, a biologically appropriate time point to assess ELAM-1-driven IDO expression.

Quantitative RT-PCR was performed to investigate changes in the expression of the induced *IDO* gene.

The promoter of ELAM-1 showed a significant increase after 30 min of inflammation and reached its maximum level in 2 h. After 4 h, the level of transcription began to decrease. Furthermore, no differences in expression were observed in cells transfected with pCMV/hIDO and pCMV/βgal plasmids and subsequently stimulated with IL-1β (2 and 5 ng/mL). This showed that while neither dose of IL-1β was effective on the CMV promoter, it did influence the activation of the ELAM-1 promoter (Fig. 1D).

The lack of statistical significance observed at the 1-h time point likely reflects the early transcriptional lag phase of ELAM-1 promoter activation, as maximal cytokine-induced transcriptional responses typically occur after 2–4 h of stimulation.

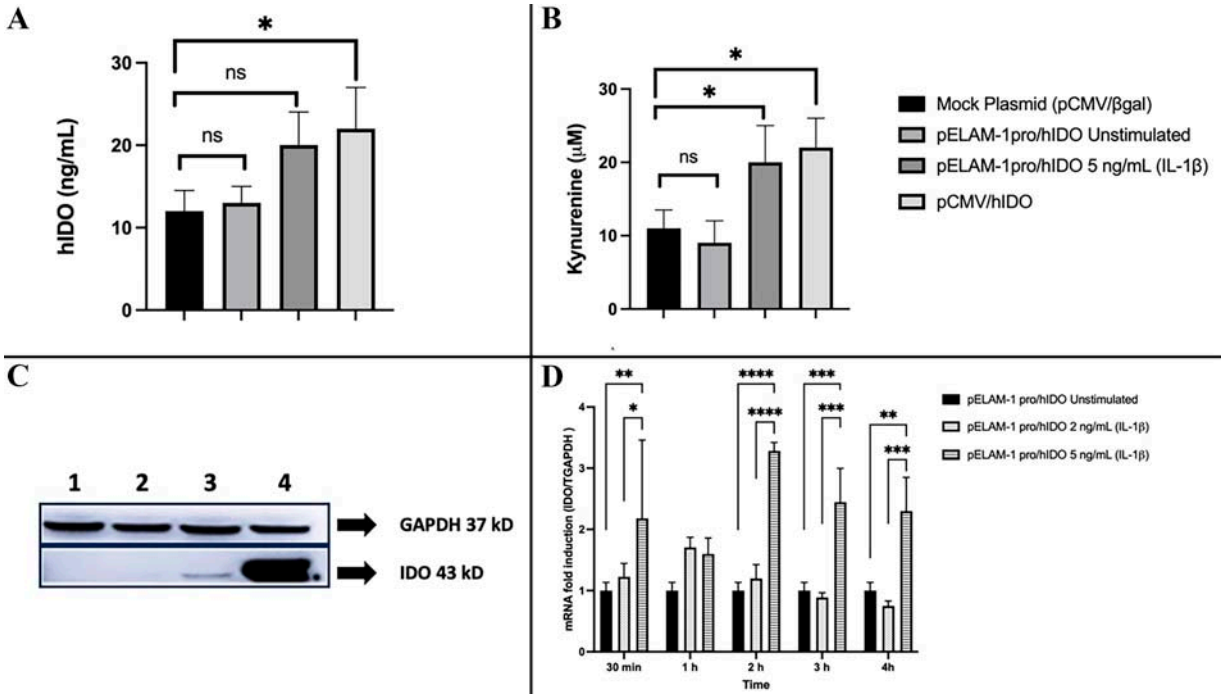

Figure 1. Inflammation-associated hIDO expression, enzymatic activity, and transcription driven by the ELAM-1 promoter in transfected HeLa cells. HeLa cells were transfected with pCMV/βgal (mock control), pELAM-1pro/hIDO (unstimulated), pELAM-1pro/hIDO stimulated with IL-1β (2 or 5 ng/mL), or constitutively active pCMV/hIDO and analyzed 24 h after transfection, unless otherwise indicated. **(A)** hIDO protein levels were quantified by ELISA. **(B)** IDO enzymatic activity was assessed by measuring L-kynurenine production. **(C)** Representative Western blot analysis showing IDO (43 kDa) and GAPDH (37 kDa). Lanes: (1) pELAM-1pro/hIDO unstimulated; (2) pELAM-1pro/hIDO + IL-1β (2 ng/mL); (3) pELAM-1pro/hIDO + IL-1β (5 ng/mL); (4) pCMV/hIDO. **(D)** Time-dependent induction of hIDO mRNA following IL-1β stimulation. Cells transfected were left unstimulated or stimulated with IL-1β (2 or 5 ng/mL) and harvested at 30 min, 1, 2, 3, and 4 h. hIDO mRNA levels were quantified by RT-qPCR, normalized to GAPDH, and expressed as a fold change relative to the unstimulated group. Data in panels A, B, and D are presented as mean ± SD from at least three independent experiments. Statistical analysis was performed using one-way ANOVA followed by Tukey's multiple comparison test. *$p < 0.05$; **$p < 0.01$; ***$p < 0.001$; ****$p < 0.0001$; ns, not significant. ELAM-1, E-selectin; ELISA, enzyme-linked immunosorbent assay; hIDO, human indoleamine 2,3-dioxygenase; IL-1β, interleukin-1β.

Therapeutic efficacy of ELAM-1-driven IDO expression in the CIA model

Clinically and histopathologically, intra-articular injection produced significant arthritis compared with previous approaches used to create RA-like arthritis. On day 14, considerable redness and swelling were observed in the right paw of mice with CIA (score 1). On day 22, injected joints had extreme redness and swelling (score 4), when compared with controls (left paw of mice) (Supplementary Fig. S4B).

Observation of the clinical response in CIA mice after treatment

The CIA mice model, previously published by our lab, was used to establish the arthritis model in BALB/c mice (Guvenc et al., 2018). This CIA mouse model underwent intra-articular gene transfer 21 days after collagen injection. The mice were regularly measured for ankle circumference. Mice treated with the plasmids pELAM-1pro/hIDO and pCMV/hIDO plasmids, in particular, showed a significant clinical improvement (notably a reduction in ankle circumference). The diagram is depicted in Figure 2.

Consistent with our previously established BALB/c local CIA model, disease severity peaked around day 21 (Guvenc et al., 2018),[39] after which treatment was administered and longitudinal clinical outcomes were monitored until day 49 to capture therapeutic effects during the chronic phase.

Following treatment, the pELAM-1pro/hIDO group exhibited a sustained reduction in ankle circumference compared with the saline and mock plasmid control groups. Statistical analysis was performed using one-way ANOVA followed by Tukey's *post hoc* test, and differences were considered statistically significant at $p < 0.05$.

Histological and immunohistochemical evaluations after treatment of the CIA model

The animals were sacrificed 28 days after treatment for histological analysis. Histological scoring was performed based on the presence of inflammation in the tissue section and ranged from 0 to 4. Inflammatory infiltration in the synovial membrane, thickening as a result of the connective tissue reaction, hyperplasia of the lining cells of the synovial membrane, development of palisade-like

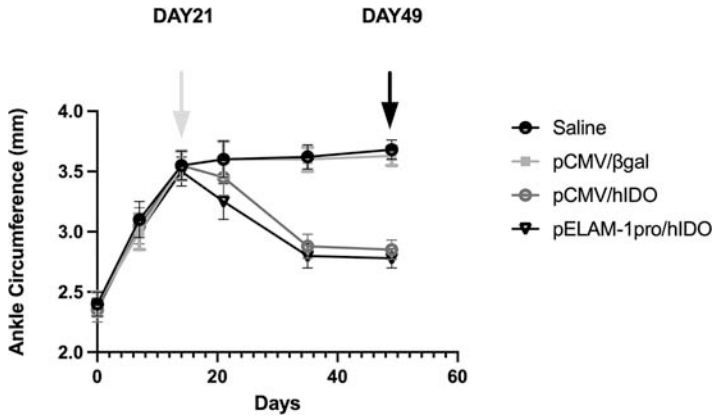

Figure 2. Therapeutic effects of intra-articular plasmid delivery on ankle swelling in the collagen-induced arthritis (CIA) model. Collagen-induced arthritis was established in mice, and intra-articular treatment was administered on day 21, corresponding to the maximum severity of the disease. Mice received pELAM-1pro/hIDO, pCMV/hIDO (constitutive expression control), pCMV/βgal (mock plasmid control), or saline. Ankle circumference was measured weekly until day 49 to monitor disease progression. Data are presented as mean ± SD. Longitudinal measurements were performed using all available animals at each time point; after day 21, the measurements reflect the remaining animals ($n = 4$ per group) until the final experimental endpoint (day 28 after treatment; CIA day 49). Each group initially included $n = 8$ mice, with 2 mice sacrificed on day 7 and 2 mice on day 21 for histological analyses. Statistical analysis was performed using one-way ANOVA followed by Tukey's multiple comparison test. The white arrow indicates the time of treatment (day 21), and the black arrow indicates the final endpoint (day 28 after treatment; CIA day 49).

patterns in the synovial membrane, presence of pannus, angiogenesis, hyperplasia of chondrocytes, and formation of new capillary vessels in cartilage tissues, formation of new capillaries in cartilage tissue just next to the synovial membrane, and cartilage damage in cartilage tissues. Histological sections were evaluated considering the parameters mentioned. Bone involvement was also assessed within the histological scoring framework, including pannus invasion at the bone–cartilage interface and preservation of cortical bone integrity. In the group treated with pELAM-1pro/hIDO, reduced pannus-associated bone erosion and improved cortical preservation were observed compared with saline and mock controls.

To further characterize *in vivo* plasmid delivery, anti-GFP immunohistochemical staining was performed on joint sections. GFP-positive cells were predominantly observed within the synovial lining layer and articular cartilage regions (Fig. 3), confirming localized transgene expression after intra-articular liposomal delivery. Due to the heterogeneous distribution inherent in liposome-mediated gene transfer, precise quantification of transfection efficiency for each individual cell type was not feasible.

On day 7, pELAM-1pro/hIDO-treated mice had a significantly lower histological score, which dropped to 2 on day 21. In mice treated with pCMV/hIDO, recovery was delayed, and the score decreased to 2 only on day 28 after treatment. No significant improvements were observed in CIA mice treated with saline and pCMV/βgal (mock/negative control) (Fig. 4).

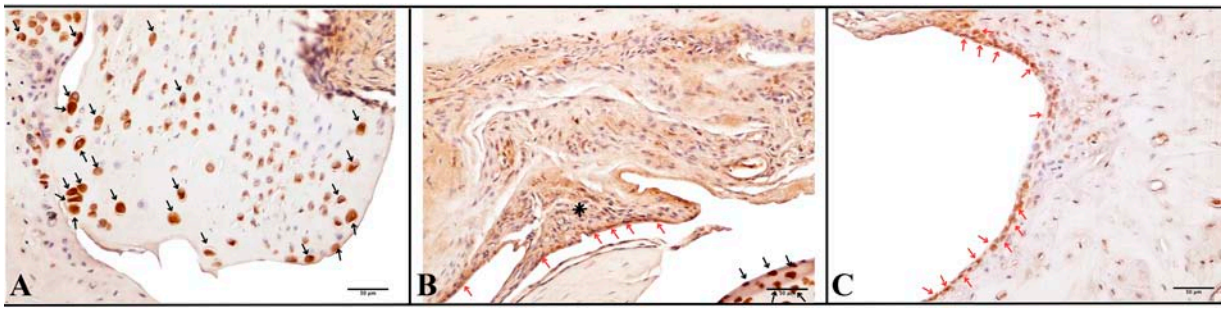

Figure 3. Liposome-mediated intra-articular pcDNA-GFP gene transfer demonstrated by GFP immunohistochemistry in CIA joints. The pcDNA-GFP plasmid (Addgene plasmid #160697) complexed with Lipofectamine 2000 was administered intra-articularly to CIA mice. Joint tissues were harvested 24 h after injection and processed for immunohistochemical detection of GFP expression using an anti-GFP antibody. **(A)** Articular cartilage demonstrating prominent nuclear 3,3′-diaminobenzidine (DAB)-positive staining in numerous chondrocytes (black arrows), indicating successful transgene expression within cartilage tissue. **(B)** Synovial membrane and subsynovial region showing GFP immunoreactivity in synovial lining cells (red arrows). Subsynovial stromal cells distributed along collagen bundles also exhibit DAB-positive staining (*), suggesting transgene expression within the synovial stroma. **(C)** Higher-magnification view of the synovial lining illustrating strong nuclear immunoreactivity of GFP in synovial lining cells (red arrows), supporting efficient gene transfer to synovial tissue. GFP expression was qualitatively evaluated in joint tissue sections from $n = 2$ mice, and representative images are shown. Immunostaining was performed using a biotin–streptavidin detection system with DAB as chromogen (brown immunoreactivity) and hematoxylin counterstaining (blue nuclei). Scale bar = 50 μm in all panels.

IDO immunoreactivity in CIA joints after intra-articular treatment

Immunohistochemical analysis was performed to evaluate *in vivo* IDO expression in ankle joints 28 days after intra-articular treatment (day 49 of the CIA protocol).

In saline-treated CIA joints (Fig. 5A), restricted endogenous IDO immunoreactivity was observed. Moderate cytoplasmic staining was detected in scattered macrophage-like cells within the subsynovial stroma, with focal IDO-positive chondrocytes in the articular cartilage. Weak immunoreactivity was also present in the basal keratinocytes of the overlying skin.

A comparable staining pattern was observed in the mock plasmid group (pCMV/βgal) (Fig. 5B), where IDO immunoreactivity remained limited to scattered synovial and subsynovial cells, focal cartilage staining, and weak epidermal positivity.

In contrast, joints treated with pELAM-1pro/hIDO (Fig. 5C) demonstrated increased IDO immunoreactivity localized predominantly to inflamed synovial regions. Strong cytoplasmic staining was observed in synovial lining cells, subsynovial stromal cells, and pannus tissue. IDO-positive chondrocytes were also detected within the articular cartilage, along with increased immunoreactivity in dermal regions adjacent to the injection site.

The group treated with the group treated with pCMV/hIDO (Fig. 5D) exhibited more widespread and diffuse cytoplasmic IDO immunoreactivity. Strong staining was observed throughout the synovial lining, subsynovial stroma, articular cartilage, and the overlying skin, consistent with constitutive promoter-driven expression.

Staining was performed using a biotin-streptavidin detection system with DAB as chromogen and hematoxylin counterstaining. Positive control staining in the tissue of the human pancreatic adenocarcinoma and rat spleen is presented in Supplementary Figure S5.

Immunohistochemical evaluation of CD68 + synovial macrophages and $CD4^+$ infiltrating lymphocytes after treatment

Semi-quantitative immunohistochemical analysis showed that pELAM-1pro/hIDO reduced macrophage and T-cell infiltration in inflamed joints throughout the post-treatment period (days 7, 21, and 28), with the most pronounced reduction observed at the final experimental endpoint (day 28 after treatment; CIA day 49). $CD68^+$ synovial macrophage scores decreased from 3.0 ± 0.0 in controls to 1.0 ± 0.4, and $CD4^+$ T-lymphocyte scores decreased from 3.0 ± 0.0 to 1.2 ± 0.3 (Fig. 6A–C).

Rapid clinical and histological improvement with pELAM-1pro/hIDO, particularly in a strain relatively resistant to CIA, supports the therapeutic potential of ELAM-1 promoter-based *IDO* delivery for localized treatment in RA. Although these findings are consistent with inflammation-associated promoter activity, in the present study, no direct *in vivo* kinetic analysis of promoter activation was performed. Early suppression of $CD4^+$ T cells and $CD68^+$ macrophages supports their mechanistic role in interrupting the inflammatory cascade before irreversible tissue damage occurs.

Local IDO immunoreactivity was demonstrated in treated joints, and the associated reductions in $CD4^+$ T-cell and $CD68^+$ macrophage infiltration are consistent with, but do not establish, IDO-mediated immunomodulation within the inflamed microenvironment.

DISCUSSION

The systemic use of biological agents in immunotherapy, while intended to reduce disease burden, has introduced new challenges including increased treatment costs and immunological side effects such as reactivation of latent infections including tuberculosis. Another factor

Figure 4. Time-dependent histological evaluation and scoring of ankle joints in treated CIA mice. **(A)** Representative hematoxylin-eosin (H&E)-stained sections of ankle joints obtained on days 7, 21, and 28 after intra-articular treatment. For histopathological evaluation, two mice per group were sacrificed on day 7 and day 21, and four mice per group at the final experimental end point (day 28 after treatment; CIA day 49). The sections were semi-quantitatively scored (0–4) based on inflammatory cell infiltration, synovial hyperplasia, pannus formation, and cartilage/bone damage. Histopathological scores are indicated below each panel. Arrows denote specific pathological features as described. (H&E staining; scale bar = 50 μm). Saline group: Day 7—Mild to moderate chondrocyte hyperplasia in the articular cartilage (↕), infiltration of inflammatory cells in the synovial membrane (∇) and slight thickening of the synovial membrane(→); Day 21—Severe infiltrations of inflammatory cells in the synovial membrane (s) and thickening due to increased connective tissue (→), new blood vessel formation in the synovial membrane (∇);Day 28—Degenerative and necrotic changes in the chondrocytes (∇), pannus formation (↑), inflammatory cell infiltrations in the synovial membrane (∇). pCMV/βgal treatment group: Day 7—Mild to moderate chondrocyte hyperplasia in the articular cartilage (⟹), inflammatory cell infiltrations in the synovial membrane (→), and new blood vessel formation in the synovial membrane (∇); Day 21—Severe inflammatory cell infiltrations in the synovial membrane (→), severe necrosis (⟹), and fibrin exudation (∇), in the joint plate and irregular chondrocyte hyperplasia (↕); Day 28—Degenerative and necrotic changes in chondrocytes (↱), severe and irregular chondrocyte hyperplasia, new capillary vascular formation in cartilage tissue (∇). pELAM-1pro/hIDO treatment group: Day 7—Slight thickening of the synovial membrane and infiltration of inflammatory cells (↘); Day 21—Mild chondrocyte hyperplasia on the cartilage surface (→), thickening due to infiltration of inflammatory cells in the synovial membrane (⟹); Day 28—Mild hyperplasia in chondrocytes (k) and thickening of synovial membrane and infiltration of inflammation cells (→). pCMV/hIDO treatment group: Day 7—Inflammatory cell infiltrations in the synovial membrane (→), severe necrosis of the chondrocytes in the joint plate (⟹); Day 21—Occasional irregular chondrocyte hyperplasia (↔), severe degenerative and necrotic changes in chondrocytes (←), severe and irregular chondrocyte hyperplasia and new vessel formation in the cartilage tissue (∇); Day 28—Mild to moderate chondrocyte hyperplasia of the articular cartilage (K), inflammatory cell infiltrations in the synovial membrane (→), and thickening of the synovial membrane (→); **(B)** semi-quantitative histological scores of ankle joints from treated CIA mice on days 7, 21 and 28 after treatment. Scores were assigned on a scale of 0 to 4 according to the severity of histopathological changes.

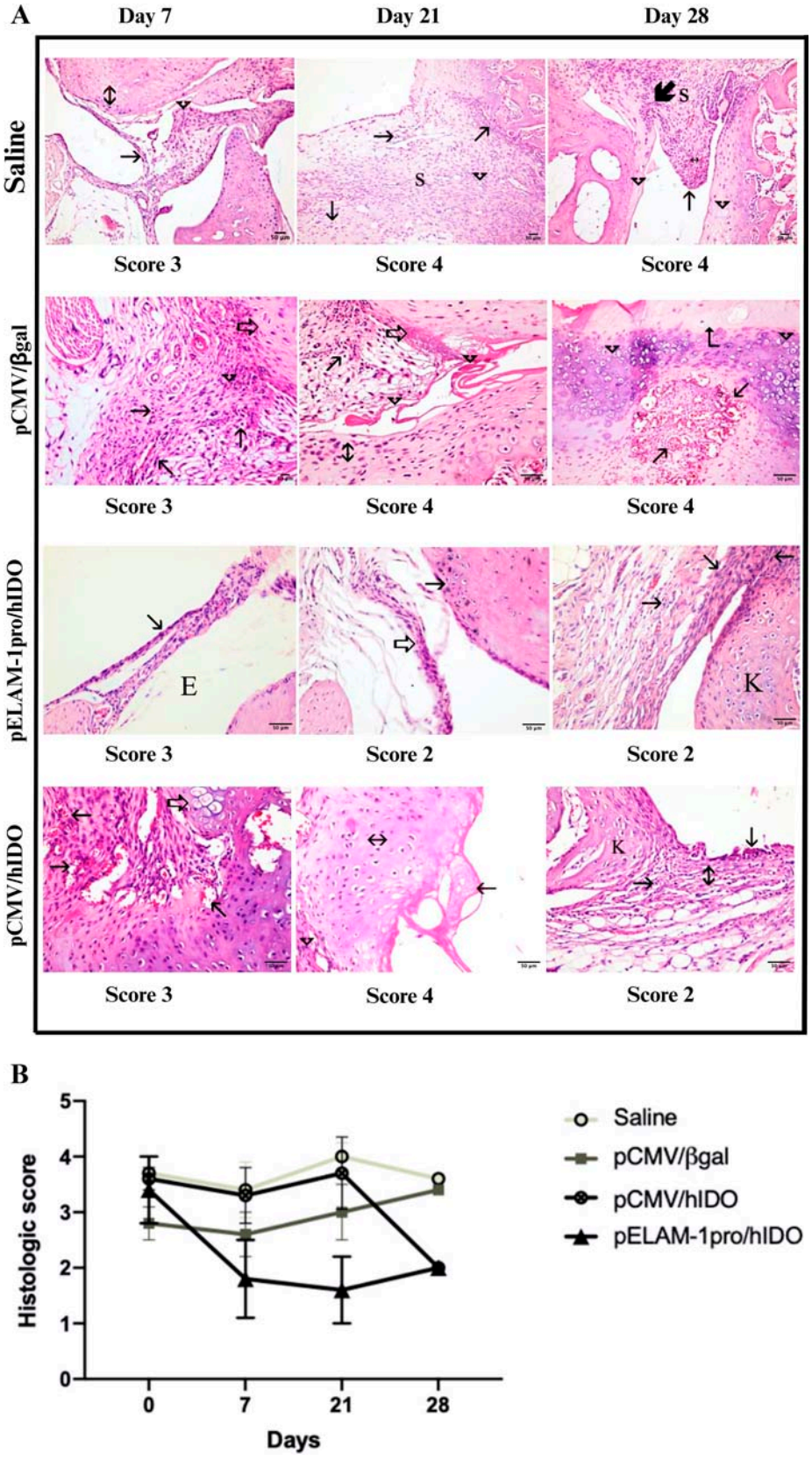
A
Day 7
Day 21
Day 28
Saline
pCMV/βgal
pELAM-1pro/hIDO
pCMV/hIDO
Score 3
Score 4
Score 4
Score 3
Score 4
Score 4
Score 3
Score 2
Score 2
Score 3
Score 4
Score 2
S
E
K
B
Histologic score
Days
0
7
21
28
Saline
pCMV/βgal
pCMV/hIDO
pELAM-1pro/hIDO

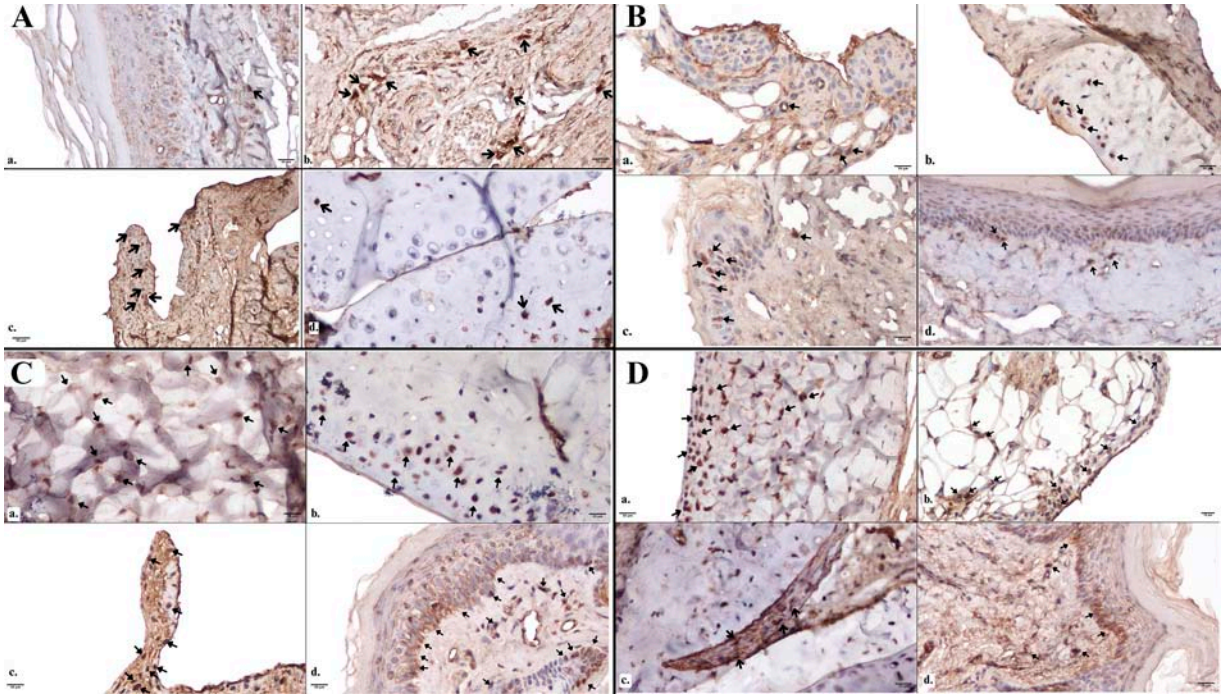

Figure 5. Immunohistochemical detection of IDO expression in CIA joints at the final experimental end point (day 28 after treatment; CIA day 49**).** Representative immunohistochemical staining of indoleamine 2,3-dioxygenase (IDO) immunoreactivity in ankle joint sections of collagen-induced arthritis (CIA) mice. IDO immunohistochemical analysis was performed at the final experimental end point using a subset of available joint tissue sections ($n = 2$ mice per group), and representative staining patterns are shown. **(A) Saline: a.** Synovial membrane and subsynovial tissue showing moderate cytoplasmic IDO immunoreactivity in scattered macrophages within the subsynovial stroma. **b.** Articular cartilage that demonstrates focal IDO-positive chondrocytes (black arrows), indicating limited IDO expression within the cartilage layer. **c.** Skin overlying the bone that exhibits weak IDO immunoreactivity in basal keratinocytes and focally in the spinous layer; the black arrow indicates a rare IDO-positive dermal cell. **d.** Higher-magnification view of the skin tissue demonstrating the sparse distribution of IDO-positive cells in the epidermal and dermal compartments. **(B) Mock treatment (pCMV/βgal): a.** Synovial membrane demonstrating IDO-positive macrophages within the subsynovial stroma, exhibiting a moderate and non-diffuse cytoplasmic staining pattern. **b.** Articular cartilage showing scattered IDO-positive chondrocytes (black arrows), consistent with limited expression of IDO in cartilage layer. **c.** Skin overlying bone showing weak IDO immunoreactivity in basal keratinocytes and rare IDO-positive cells at the epidermis–dermis junction. **d.** Dermal connective tissue showing sparse IDO-positive inflammatory cells with focal, mild cytoplasmic immunoreactivity. **(C) pELAM-1pro/hIDO treatment: a.** Articular cartilage demonstrating chondrocytes with strong cytoplasmic IDO immunoreactivity (black arrows). **b.** Synovial membrane showing numerous strongly IDO-positive macrophages within the synovial stroma (black arrows). **c.** Pannus tissue overlying the articular surface exhibiting moderate IDO immunoreactivity; black arrows indicate IDO-positive cells within the pannus. **d.** Skin overlying the bone exhibiting an increased density of IDO-positive cells in the basal epidermal layer, with additional IDO-positive cells distributed within the dermis (black arrows). **(D) pCMV/hIDO treatment: a.** Articular cartilage demonstrating numerous strongly IDO-positive chondrocytes (black arrows). **b.** Subsynovial tissue showing intense IDO immunoreactivity in stromal cells and along septa between adipocyte clusters (black arrows). **c.** Synovial membrane from a pCMV/hIDO-treated joint exhibiting diffuse and strong IDO immunoreactivity along the synovial lining (black arrows). **d.** Skin overlying the bone displaying diffuse IDO immunoreactivity in both the epidermis and dermis, with numerous IDO-positive cells along the dermal–epidermal junction and within the dermis (black arrows). Staining was performed using a biotin–streptavidin detection system with DAB as chromogen and hematoxylin counterstaining. Original magnification ×400. (Scale bar = 50 μm in all panels).

driving up treatment costs is the short half-life of these biologics, which require regular injections. Alternatively, therapeutic genes could be delivered systemically and/or topically to the site of inflammation.

Our findings suggest that intra-articular delivery of a plasmid carrying the *hIDO* gene under the control of the ELAM-1 promoter is associated with the amelioration of arthritis in a mouse model with CIA.

All *in vivo* experiments were conducted using male BALB/c mice. Although RA in humans shows a female predominance, the sexual dimorphism in murine CIA models is highly strain-dependent and context-dependent.[42] Previous reports have demonstrated that, particularly in certain CIA settings, male mice can exhibit earlier onset and greater cumulative disease severity compared with females.[43,44] In our experimental system, supplementary observations similarly indicated that arthritis development and therapeutic response in female BALB/c mice occurred later and with lower clinical severity compared with males. Because the primary objective of this study was to evaluate inflammation-dependent promoter activation and therapeutic efficacy at peak disease, male cohorts were selected to ensure a robust and synchronized inflammatory window. Therefore, the use of male mice reflects a methodological choice aligned with both published CIA literature and our own experimental observations, rather than an oversight of sex as a biological variable.

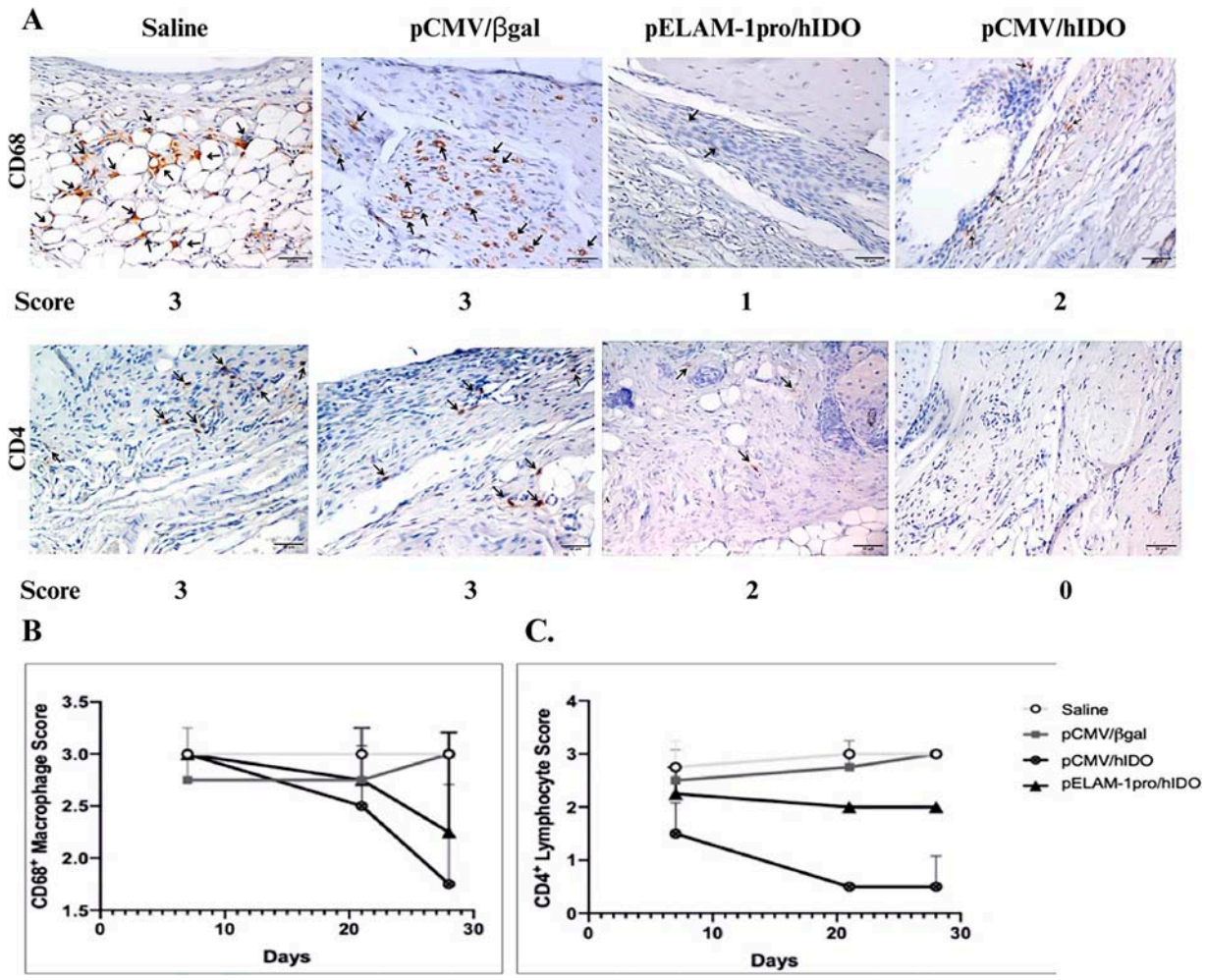

Figure 6. Immunohistochemical evaluation of synovial macrophage and T-cell infiltration in CIA joints. **(A)** Representative immunohistochemical staining of ankle joint sections showing CD68+ synovial macrophages and CD^+ infiltrating lymphocytes in saline, pCMV/βgal (mock plasmid), pCMV/hIDO, and pELAM-1pro/hIDO–treated groups at the final experimental endpoint (day 28 after treatment; CIA day 49). Panel A shows representative images from the final experimental endpoint. Arrows indicate positively stained cells. (Hematoxylin counterstain; scale bar = 50 μm). **(B)** Semi-quantitative immunohistochemical scores of $CD68^+$ synovial macrophage infiltration on days 7, 21, and 28 after treatment. **(C)** Semi-quantitative immunohistochemical scores of $CD4^+$ T lymphocyte infiltration on days 7, 21, and 28 after treatment. For day 7 and day 21, joint sections of $n = 2$ mice per group were evaluated; at the final experimental endpoint (day 28 after treatment; CIA day 49), joint sections of $n = 4$ mice per group were analyzed. All evaluations were performed independently by two blinded observers using a scoring system of 0–3 (0 = none, 1 = mild, 2 = moderate, 3 = severe). Data are presented as mean ± SD.

The H2q haplotype (present in DBA/1 mice) is frequently used in investigations to mimic arthritis in animal subjects. It is well established that mice with the C57BL/6 or BALB/c H2q haplotype are the least receptive to immunization with collagen and adjuvant. However, it has been demonstrated by the use of modeling methods and high-dose adjuvants and timing in non-responsive mice that CIA can be induced.[45] Furthermore, we previously demonstrated that BALB/c mice can develop local arthritis within a week after receiving intra-articular collagen and subcutaneous CFA.[39] However, the severity of arthritis development in this model can vary from mouse to mouse, making it more suitable for studying the therapeutic effect than the preventive characteristic. In this study, mice with a clinical arthritis score of 3 were selected for treatment. The CIA model is widely used to evaluate gene therapy approaches in experimental settings.

Gene therapies are based on *ex vivo* cellular therapies or *in vivo* injection of genes as plasmids or viral vectors. Antigen-specific allogenic APCs or T cells and/or genetically modified allogenic fibroblasts are frequently utilized in *ex vivo* cellular treatments, the latter often being modified with retroviral gene delivery systems to provide tolerance in the lymph node and synovial membrane. According to several studies, all developed *ex vivo* or *in vivo* gene therapies can be administered locally (intra-articular or peri-articular) or systemically (intramuscular or intravenous).[46] Furthermore, Bandara and colleagues[38] performed the first intra-articular gene transfer in an animal model with RA and observed that intra-articular injection has more advantages than other administration methods. They can easily penetrate the synovium during intra-articular injections of genes or genetically modified

cells. In comparison to systemic injections, intra-articular injections allow for the use of lower amounts of gene or viral vectors, and this system allows for the transfection of more target cells in joints. In addition, due to low mitotic ratios of fibroblast-like synoviocytes after intra-articular injections, long-term expression of transgenes can be obtained.

In line with these advantages, we employed a non-viral liposomal plasmid system for intra-articular delivery to further enhance local bioavailability while minimizing systemic exposure and vector-related immunogenicity. This approach provides transient, but therapeutically sufficient, gene expression and offers a safer and more clinically translatable alternative to viral vectors. Although the observed *in vivo* gene transfer efficiency (approximately 20%–30%) may appear modest, heterogeneous transfection is an expected feature of intra-articular liposome-mediated plasmid delivery. GFP immunohistochemistry confirmed transgene expression within key joint compartments, including synovial lining cells and articular chondrocytes. Notably, significant clinical and histological improvement was achieved despite partial cellular transduction, indicating that complete transfection of all joint-resident cells is not required to obtain therapeutic benefit in this localized model.

In most of the genetic therapy approaches, IL-1 antagonists, TNF-α antagonists, IL-4, IL-10, IFN-γ, TGF-α, ICAM, CD44, IGF-1, bFGF, HGF, FasL, NF-kB, and IDO are candidate genes for RA gene therapies.[38,45–49] The therapeutic approach we used addresses a significant limitation of conventional systemic treatments for RA: the risk of widespread immunosuppression and associated side effects, such as reactivation of latent infections.[45] Using the ELAM-1 promoter, which is known to respond to pro-inflammatory cytokines such as IL-1 and TNF-α,[22,23] we observed a localized pattern of IDO immunoreactivity in inflamed joints. This distribution is consistent with localized promoter-driven transgene expression in inflamed tissues, although the intermediate *in vivo* steps that link inflammatory activation, promoter activity, and transgene expression were not directly examined in the present study.

Intra-articular injection of a lentiviral vector carrying the IL-10 gene under the control of the inflammation-inducing Saa3 and Mmp13 promoters yielded similar results.[47] Compared to other inflammation-responsive promoters previously used in arthritis gene therapy, the ELAM-1 promoter has been reported to exhibit relatively more restricted spatial and temporal activation patterns. Promoters such as Saa3 can be broadly activated during systemic acute-phase responses, while Mmp13 activity is mainly associated with later stages of cartilage degradation. In contrast, ELAM-1 was induced in activated endothelial cells in response to pro-inflammatory cytokines under inflammatory conditions. For an immunomodulatory enzyme such as IDO, coupling expression with inflammatory signaling can reduce the risk of widespread or prolonged systemic immunosuppression. Therefore, the ELAM-1 promoter was selected to favor inflammation-associated and spatially restricted immunomodulatory activity compared with constitutive promoter systems.

Based on this rationale, we used IDO as a tolerance-inducing gene under the control of the ELAM-1 promoter. Because the ELAM-1 promoter is responsive to inflammatory signals, it can enable IDO transcription during active inflammatory phases and, thus, support local immunomodulation early in disease progression. This is because the ELAM-1 promoter region is easily activated. Some studies demonstrated that IL-10 can boost production of TNF-α in response to immune complexes and FcRI and FcRIIa expression, particularly on monocytes and macrophages.[46] This may lead to long-term exacerbation of arthritis. Therefore, it was thought that the use of a central role therapeutic gene such as IDO instead of IL-10 may be more useful. However, the most important potential problem with IDO, which we aim to use as a potential therapeutic gene, is the possibility that IDO may suppress the excitability of the ELAM-1 promoter. There are no published data that clearly and definitively show that IDO suppresses the ELAM-1 promoter. It is also possible that IDO may be an effective, albeit transient, immune regulator until the ELAM-1 promoter is suppressed. To test this possibility, we investigated whether CAT expression would be affected in HeLa cells co-transfected with a pELAM-1pro/CAT plasmid and a CMV promoter control plasmid that constitutively provides IDO expression. In these experiments, pCMV/βgal was used as a control plasmid instead of pCMV/IDO. IDO expression did not appear to repress ELAM-1 promoter activity and was associated with an increase in promoter activity.

In the first study on *IDO* gene therapy in RA and/or CIA models,[50] it was shown that the adenovirus-mediated transduction of the *IDO* gene under the control of the constitutive CMV promoter to the affected joint region in rats with CIA resulted in a significant clinical and histological improvement, as well as a decrease in synovial IL-17 levels, elimination of $CD4^+$ T cells infiltrating the synovium by apoptosis and suppression of $CD68^+$ synovial macrophages. Consistent with this work, in our study, the clinical and histological scores, as well as the ankle circumference measurements (Figs. 2 and 4), showed a marked improvement in mice treated with pELAM-1pro/hIDO. A particularly notable finding was the earlier therapeutic response observed in this group, with a significant reduction in histological score on day 7 after treatment, while mice treated with the constitutively active CMV promoter-controlled plasmid (pCMV/hIDO) showed comparatively delayed recovery. Therefore, the ELAM-1 promoter was

selected to favor inflammation-associated and spatially restricted immunomodulatory activity compared with constitutive promoter systems.

In addition, bone involvement was evaluated as part of the histopathological scoring of H&E-stained sections. The scoring criteria included the assessment of pannus invasion at the bone–cartilage interface, cortical bone integrity, and preservation of periarticular bone structures. In the group treated with pELAM-1pro/hIDO, reduced pannus-associated bone erosion and improved preservation of cortical architecture were observed compared with saline and mock controls, indicating that attenuation of inflammation was accompanied by secondary protection against bone destruction.

Furthermore, our immunohistochemical analysis provides crucial mechanistic insight into the observed clinical improvements. The significant decrease in $CD4^+$ T lymphocytes and $CD68^+$ macrophages in the synovial tissue of mice treated with pELAM-1pro/hIDO and pCMV/hIDO (Fig. 6) is consistent with the therapeutic effect on the known immunosuppressive functions of IDO. IDO-mediated tryptophan catabolism has been shown to induce T-cell apoptosis and suppress proliferation, while also affecting macrophage function.[16,17,21] Our findings extend this by showing that a disease-inducible system can achieve a similar, potentially faster, therapeutic outcome.

Baseline CIA joints exhibited restricted endogenous expression of IDO primarily within synovial macrophages and occasional chondrocytes, consistent with previous reports indicating that IDO is upregulated as a counter-regulatory mechanism in chronically inflamed rheumatoid joints.[51–54] Both pELAM-1pro/hIDO and pCMV/hIDO treatments were associated with increased IDO immunoreactivity within these key inflammatory cell populations, which are central mediators of joint pathology.[52–54]

ELAM-1-driven expression was predominantly localized to inflamed synovial and cartilage regions, suggesting spatially restricted transgene expression in inflamed tissues. In contrast, CMV-driven expression resulted in a broader and more diffuse distribution across the synovium, cartilage, subsynovial tissue, and the overlying skin, consistent with constitutive promoter activity.[55]

In addition, IDO-positive cells were detected in epidermal and dermal regions surrounding needle entry sites, indicating localized immunoreactivity in areas directly exposed to intra-articular injection. The detection of IDO-positive cells together with GFP-confirmed transduction patterns supports successful intra-articular gene transfer and local transgene expression rather than exclusive endogenous inflammatory induction.[56]

Further, the *IDO* gene was transcribed under the control of the CMV promoter region, transfected using an adenovirus system, and applied via intra-articular injection to locally formed arthritis joints in the first study of *IDO* gene therapy in RA and/or CIA models.[50] Our investigation employing the CIA mice model found similar outcomes when we used pELAM-1pro/hIDO plasmids for intra-articular liposome-mediated gene transfers as therapy. In addition, we found that 20%–30% of transfection attempts in joint sections were successful when plasmids were mixed with non-immunogenic liposomes as a gene delivery technique; this is comparable to the success rates seen in intra-articular liposome-mediated gene transfers in prior research.[57]

Although serial quantification of IDO would provide additional kinetic details, the primary objective of Figure 2 was to evaluate longitudinal clinical outcomes. As shown in Figure 2, intra-articular treatment resulted in significant clinical improvement. Histological follow-up at multiple time points (Fig. 4) confirmed sustained therapeutic effects. Moreover, endpoint immunohistochemical analysis on day 49 demonstrated increased local IDO immunoreactivity in treated joints (Fig. 5), supporting biologically relevant transgene expression *in vivo*.

Despite these promising results, we acknowledge a limitation in the current gene therapy strategy. As noted in a previous discussion, intra-articular injection of these plasmids is not antigen-specific, potentially affecting all cells in the joint region.

However, the use of an inflammation-responsive promoter may partially mitigate this concern by favoring transgene expression under inflammatory conditions, although complete cell-type specificity cannot be assumed. Although detailed cytokine profiling and *in vivo* kinetic analysis of IDO expression would provide further mechanistic clarification, the present study primarily aimed to evaluate inflammation-responsive promoter function and therapeutic outcomes. Due to the very limited volume of synovial fluid available from murine CIA joints, multiplex cytokine measurements (*e.g.,* TNF-α and IL-6) were not sufficiently reproducible for inclusion in the present study.

Future studies could explore more sophisticated delivery systems or promoter designs to achieve even greater specificity. Long-term studies are also warranted to assess the durability of the therapeutic effect and monitor potential side effects.

In conclusion, our study validates the therapeutic potential of *IDO*-based local gene delivery and extends this approach by employing an inflammation-responsive ELAM-1 promoter. The findings support localized therapeutic effects in this model and are consistent with inflammation-associated promoter activity, while also

highlighting the need for future studies to address *in vivo* promoter kinetics and pharmacodynamic readouts.

AUTHORS' CONTRIBUTIONS

H.B.O. conceptualized and supervised the work. F.E. and M.K. performed molecular cloning, generated the plasmids. M.K., İ.Y., and A.Ö.B.S. conducted all in vitro work. M.K., G.G.-B., and M.Y. performed and/or supervised all animal work. C.G.Ö.A. and A.A. performed and evaluated histopathological and immunohistochemical analyses. A.Y.O. conducted all biochemical analyses and evaluated. M.K. wrote and revised the article. H.B.O. reviewed and edited the article. All authors approved the final article.

AUTHOR DISCLOSURE

The authors declare no competing interests.

FUNDING INFORMATION

This study was supported by the Scientific and Technical Research Council of Türkiye (TUBITAK-COST Project No: 113S375) under Cost Action BM1305 [Action to Focus and Accelerate Cell-based Tolerance-inducing Therapies (A FACTT)]. COST is supported by the EU Framework Program Horizon 2020.

SUPPLEMENTARY MATERIAL

Supplementary Figures

REFERENCES

1. McInnes IB, Schett G. The pathogenesis of rheumatoid arthritis. N Engl J Med 2011;365(23): 2205–2219; doi: 10.1056/NEJMRA1004965
2. Mellado M, Martinez-Munoz L, Cascio G, et al. T cell migration in rheumatoid arthritis. Front Immunol 2015;6:384; doi: 10.3389/fimmu.2015.00384
3. Shen F, Gaffen SL. Structure-function relationships in the IL-17 receptor: Implications for signal transduction and therapy. Cytokine 2008; 41(2):92–104; doi: 10.1016/j.cyto.2007.11.013
4. Onishi RM, Gaffen SL. Interleukin-17 and its target genes: Mechanisms of IL-17 function in disease. Immunology 2010;129(3):311–321; doi: 10.1111/j.1365-2567.2009.03240.x
5. Aletaha D, Smolen JS. Diagnosis and management of rheumatoid arthritis: A review. JAMA 2018;320(13):1360–1372; doi: 10.1001/jama.2018.13103
6. Emery P, Bingham CO, Burmester GR, et al. Certolizumab pegol plus methotrexate in early RA (C-EARLY). Ann Rheum Dis 2017;76(1):96–104; doi: 10.1136/annrheumdis-2015-209057
7. Breedveld FC, Weisman MH, Kavanaugh AF, et al. The PREMIER study. Arthritis Rheum 2006; 54(1):26–37; doi: 10.1002/art.21519
8. Mandema JW, Salinger DH, Baumgartner SW, et al. Dose-response meta-analysis of biologics in rheumatoid arthritis. Clin Pharmacol Ther 2011;90(6):828–835; doi: 10.1038/clpt.2011.256
9. Liu S, Kiyoi T, Takemasa E, et al. Intra-articular lentivirus-mediated gene therapy targeting CRACM1. J Pharmacol Sci 2017;133(3):130–138; doi: 10.1016/j.jphs.2017.02.001
10. Munn DH, Zhou M, Attwood JT, et al. Prevention of allogeneic fetal rejection by tryptophan catabolism. Science 1998;281(5380):1191–1193; doi: 10.1126/science.281.5380.1191
11. Mellor AL, Baban B, Chandler P, et al. Induced indoleamine 2,3-dioxygenase expression suppresses T cell clonal expansion. J Immunol 2003;171(4):1652–1655; doi: 10.4049/jimmunol.171.4.1652
12. Gurtner GJ, Newberry RD, Schloemann SR, et al. Inhibition of indoleamine 2,3-dioxygenase augments TNBS colitis. Gastroenterology 2003; 125(6):1762–1773; doi: 10.1053/j.gastro.2003.08.031
13. Hayashi T, Beck L, Rossetto C, et al. Inhibition of experimental asthma by indoleamine 2,3-dioxygenase. J Clin Invest 2004;114(2):270–279; doi: 10.1172/JCI21275
14. Kwidzinski E, Bunse J, Aktas O, et al. Indoleamine 2,3-dioxygenase is expressed in the CNS and down-regulates autoimmune inflammation. Faseb J 2005;19(10):1347–1349; doi: 10.1096/fj.04-3228fje
15. Beutelspacher SC, Tan PH, McClure MO, et al. Expression of indoleamine 2,3-dioxygenase by endothelial cells. Am J Transplant 2006;6(6): 1320–1330; doi: 10.1111/j.1600-6143.2006.01324.x
16. Munn DH, Shafizadeh E, Attwood JT, et al. Inhibition of T cell proliferation by macrophage tryptophan catabolism. J Exp Med 1999;189(9): 1363–1372; doi: 10.1084/jem.189.9.1363
17. Mellor AL, Keskin DB, Johnson T, et al. Cells expressing indoleamine 2,3-dioxygenase inhibit T cell responses. J Immunol 2002;168(8): 3771–3776; doi: 10.4049/jimmunol.168.8.3771
18. Fallarino F, Grohmann U, Vacca C, et al. T cell apoptosis by tryptophan catabolism. Cell Death Differ 2002;9(10):1069–1077; doi: 10.1038/sj.cdd.4401073
19. Frumento G, Rotondo R, Tonetti M, et al. Tryptophan-derived catabolites inhibit T and NK cell proliferation. J Exp Med 2002;196(4):459–468; doi: 10.1084/jem.20020121
20. Bauer TM, Jiga LP, Chuang JJ, et al. Immunosuppressive role of indoleamine 2,3-dioxygenase. Transpl Int 2005;18(1):95–100; doi: 10.1111/j.1432-2277.2004.00031.x
21. Wu H, Gong J, Liu Y. Indoleamine 2,3-dioxygenase regulation of immune response. Mol Med Rep 2018;17(4):4867–4873; doi: 10.3892/mmr.2018.8537
22. Pober JS, Gimbrone MA, Lapierre LA, et al. Overlapping patterns of activation of human endothelial cells. J Immunol 1986;137(6):1893–1896.
23. Wellicome SM, Thornhill MH, Pitzalis C, et al. A monoclonal antibody detecting TNF/IL-1-induced endothelial antigen. J Immunol 1990; 144(7):2558–2565.
24. Kluger MS, Johnson DR, Pober JS. Sustained E-selectin expression mechanisms. J Immunol 1997;158(2):887–896.
25. Gompels LL, Madden L, Lim NH, et al. In vivo fluorescence imaging of E-selectin. Arthritis Rheum 2011;63(1):107–117; doi: 10.1002/art.30082
26. Jaggar RT, Chan HY, Harris AL, et al. Endothelial cell-specific TNF-alpha expression using E-selectin promoter. Hum Gene Ther 1997;8(18): 2239–2247; doi: 10.1089/hum.1997.8.18-2239
27. Walton T, Wang JL, Ribas A, et al. Endothelium-specific expression of an E-selectin promoter recombinant adenoviral vector. Anticancer Res 1998;18(3A):1357–1360.
28. Maxwell IH, Kaletta C, Naujoks K, et al. Targeting diphtheria toxin A-chain transcription to activated endothelial cells. Angiogenesis 2003; 6(1):31–38; doi: 10.1023/A:1025894616613

29. Garaulet G, Alfranca A, Torrente M, et al. IL-10 released by an inflammation-regulated lentiviral system attenuates arthritis. Mol Ther 2013; 21(1):119–130; doi: 10.1038/mt.2012.131

30. Trentham DE, Townes AS, Kang AH. Autoimmunity to type II collagen. J Exp Med 1977; 146(3):857–868; doi: 10.1084/jem.146.3.857

31. Wooley PH, Luthra HS, Griffiths MM, et al. Type II collagen-induced arthritis in mice. J Immunol 1985;135(4):2443–2451.

32. Wooley PH. Collagen-induced arthritis in the mouse. Methods Enzymol 1988;162:361–373; doi: 10.1016/0076-6879(88)62091-X

33. Young E, Gould D, Hart S. Toward gene therapy in rheumatoid arthritis. Expert Rev Precis Med Drug Dev 2020;5(3):123–133; doi: 10.1080/23808993.2020.1736942

34. Tsitrouli Z, Akritidou MA, Genitsaris S, et al. Gene therapy applications in rheumatoid arthritis. BioTech 2021;10(3):11; doi: 10.3390/biotech10030011

35. Evans CH, Ghivizzani SC, Robbins PD. Osteoarthritis gene therapy in 2022. Curr Opin Rheumatol 2023; 35(1):37–43; doi: 10.1097/BOR.0000000000000918

36. Selich A, Fleischauer J, Roepke T, et al. Inflammation-inducible promoters to overexpress immune inhibitory factors. Stem Cell Res Ther 2023;14:35; doi: 10.1186/s13287-023-03501-6

37. Samikkannu T, Saiyed ZM, Rao KVK, et al. Differential regulation of indoleamine-2,3-dioxygenase by HIV Tat. AIDS Res Hum Retroviruses 2009; 25(3):329–335; doi: 10.1089/aid.2008.0225

38. Bandara G, Mueller GM, Galea-Lauri J, et al. Intraarticular expression of IL-1 receptor antagonist by gene transfer. Proc Natl Acad Sci USA 1993;90(22):10764–10768; doi: 10.1073/pnas.90.22.10764

39. Guvenc G, Karacay M, Akkoc A, et al. A new protocol for collagen-induced local arthritis model in BALB/c mice. Turk J Immunol 2018; 6(1):30–36; doi: 10.25002/TJI.2018.771

40. Zhang T, Tan XL, Xu Y, et al. Expression and prognostic value of indoleamine 2,3-dioxygenase in pancreatic cancer. Chin Med J (Engl) 2017; 130(6):710–716; doi: 10.4103/0366-6999.201613

41. Thomas S, DuHadaway J, Prendergast GC, et al. Specific in situ detection of murine indoleamine 2,3-dioxygenase. J Cell Biochem 2014; 115(2):391–396; doi: 10.1002/jcb.24674

42. Dong W, Tian C, Li ZG, et al. Variation of sexual dimorphism and asymmetry in disease expression of inflammatory arthritis among laboratory mouse models with different genomic backgrounds. Lab Anim Res 2023;39(1):35; doi: 10.1186/s42826-023-00185-0

43. Schuh BM, Macáková K, Feješ A, et al. Sex differences in long-term effects of collagen-induced arthritis in middle-aged mice. Front Physiol 2023;14:1195604; doi: 10.3389/fphys.2023.1195604

44. Marinov L, Mangarov I, Nikolova I. Gender differences in collagen-induced arthritis (CIA) in mice. Biotechnol Biotechnol Equip 2021;35(1):1899–1905; doi: 10.1080/13102818.2022.2027815

45. Reinecke J, Koch H, Meijer H, et al. Current status of gene therapy for rheumatoid arthritis. BioDrugs 1999;11(2):103–114.

46. van de Loo FAJ, Smeets RL, van den Berg WB. Gene therapy in animal models of rheumatoid arthritis. Arthritis Res Ther 2004;6(5):183; doi: 10.1186/ar1214

47. Vermeij EA, Broeren MGA, Bennink MB, et al. Disease-regulated local IL-10 gene therapy diminishes synovitis. Ann Rheum Dis 2015; 74(11):2084–2091; doi: 10.1136/annrheumdis-2014-205223

48. Henningsson L, Eneljung T, Jirholt P, et al. Disease-dependent local IL-10 production ameliorates collagen-induced arthritis. PLoS One 2012; 7(11):e49731; doi: 10.1371/journal.pone.0049731

49. Evans CH, Ghivizzani SC, Robbins PD. Arthritis gene therapy and its path into the clinic. Transl Res 2013;161(4):205–216; doi: 10.1016/j.trsl.2013.01.002

50. Chen SY, Wu CL, Lai MD, et al. Amelioration of rat collagen-induced arthritis by IDO gene therapy. Hum Gene Ther 2011;22(2):145–154; doi: 10.1089/hum.2009.217

51. Williams RO. Exploitation of the IDO pathway in the therapy of rheumatoid arthritis. Int J Tryptophan Res 2013;6(Suppl 1):67–73; doi: 10.4137/IJTR.S11737

52. Yanni G, Whelan A, Feighery C, et al. Synovial tissue macrophages and joint erosion in rheumatoid arthritis. Ann Rheum Dis 1994;53(1): 39–44; doi: 10.1136/ard.53.1.39

53. Kinne RW, Brauer R, Stuhlmuller B, et al. Macrophages in rheumatoid arthritis. Arthritis Res 2000;2(3):189–202; doi: 10.1186/ar86

54. Tu J, Wang X, Gong X, et al. Synovial macrophages in rheumatoid arthritis: The past, present, and future. Mediators Inflamm 2020;2020: 1583647; doi: 10.1155/2020/1583647

55. Lee W, Nims RJ, Savadipour A, et al. Inflammatory signaling sensitizes Piezo1 mechanotransduction in articular chondrocytes. Proc Natl Acad Sci U S A 2021;118:e2001611118; doi: 10.1073/pnas.2001611118

56. Abe S, Nochi H, Ito H. Human articular chondrocytes induce interleukin-2 nonresponsiveness. Cartilage 2017;8:300–306; doi: 10.1177/1947603516661820

57. Oligino TJ, Yao Q, Ghivizzani SC, et al. Vector systems for gene transfer to joints. Clin Orthop Relat Res 2000;379(379 Suppl):S17–S30.

Received for publication September 14, 2025;
accepted after revision April 24, 2026.

Published online: May 28, 2026.